Searches for dark matter at accelerators
6/02/2019

- **Program**
  - Signatures and features
  - Searches at LEP
  - Searches at LHC
  - Comparison to direct/indirect detection results

- **Literature:**
  - Ed. by G. Bertone, *Particle Dark Matter*, Cambridge University Press (2010), Part III
  - Felix Kahlhoefer, *Review of LHC Dark Matter Searches*, Int. J. Mod. Phys. A32 (2017) 1730006
  - ALEPH, DELPHI, L3, OPAL, SLD, LEP Electroweak Working Group, SLD Electroweak Group and SLD Heavy Flavour Group Collaborations, *Precision electroweak measurements on the Z resonance*, Phys. Rept. 427 (2006) 257 and arXiv:hep-ex/0509008.
  - ATLAS Collaboration, *Search for new phenomena in final states with an energetic jet and large missing transverse momentum in pp collisions at* $\sqrt{s} = 13\,TeV$ *using the ATLAS detector*, Phys. Rev. D 94, 032005 (2016) and arXiv:1604.07773
  - CMS Collaboration, *Search for dark matter produced in association with a Higgs boson decaying to* $\gamma\gamma$ *or* $\tau^+\tau^-$ *at* $\sqrt{s} = 13\,TeV$, JHEP 09 (2018) 046 and arXiv:1806.04771

- **Material for the lecture:**

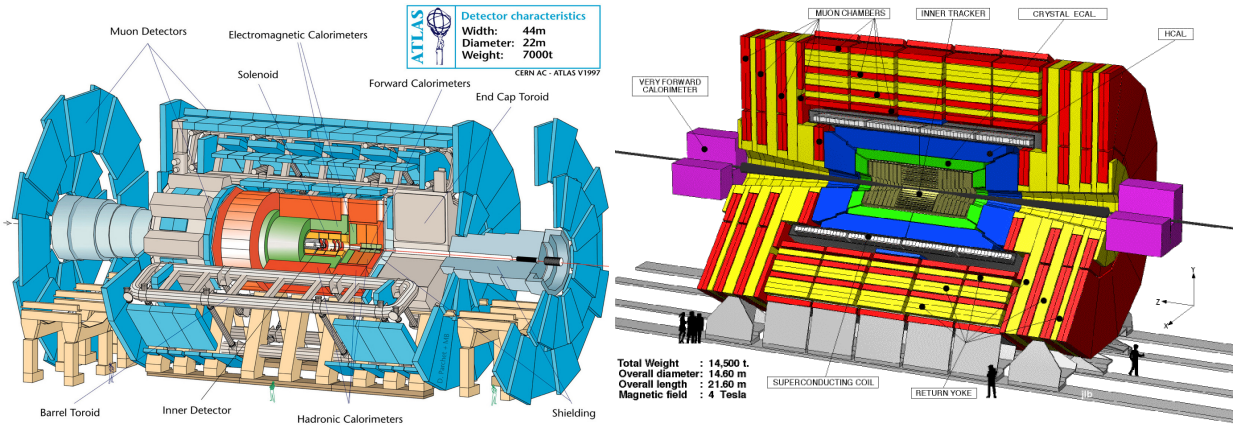

Figure 1: Schematic view of the Atlas (left) and the CMS (right) detectors. Figures from collaboration homepages.

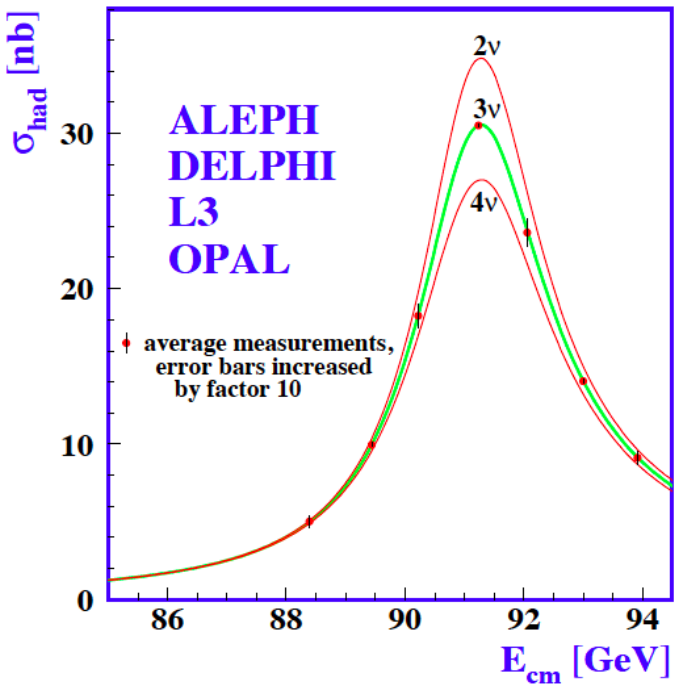

Figure 2: Measurements of the hadron production cross-section around the Z resonance. The lines represent the predicted cross-section for two, three and four neutrino species with SM coupling and negligible masses. Figure from Phys. Rept. 427 (2006) 257 and arXiv:hep-ex/0509008.

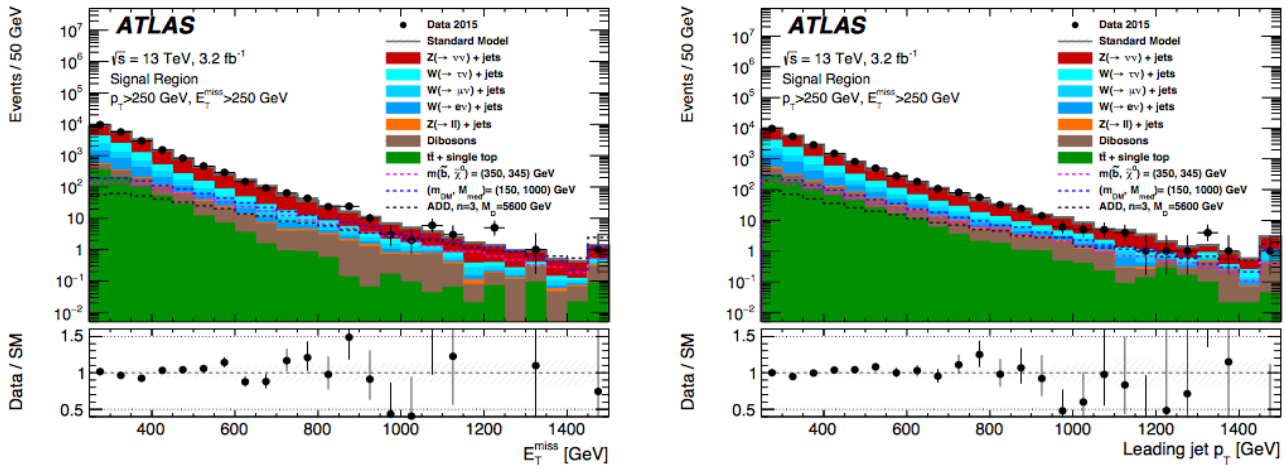

Figure 3: Measured distributions of E_T^{miss} and leading jet p_T for the lowest energy range considered in the analysis compared to the standard model expectations (coloured regions). For illustration, the distributions for different DM scenarios: extra dimensions, SUSY and WIMP, are also included (dashed lines). Figures from ATLAS Collaboration, PRD 94, 032005, 2016 or arXiv:1604.07773

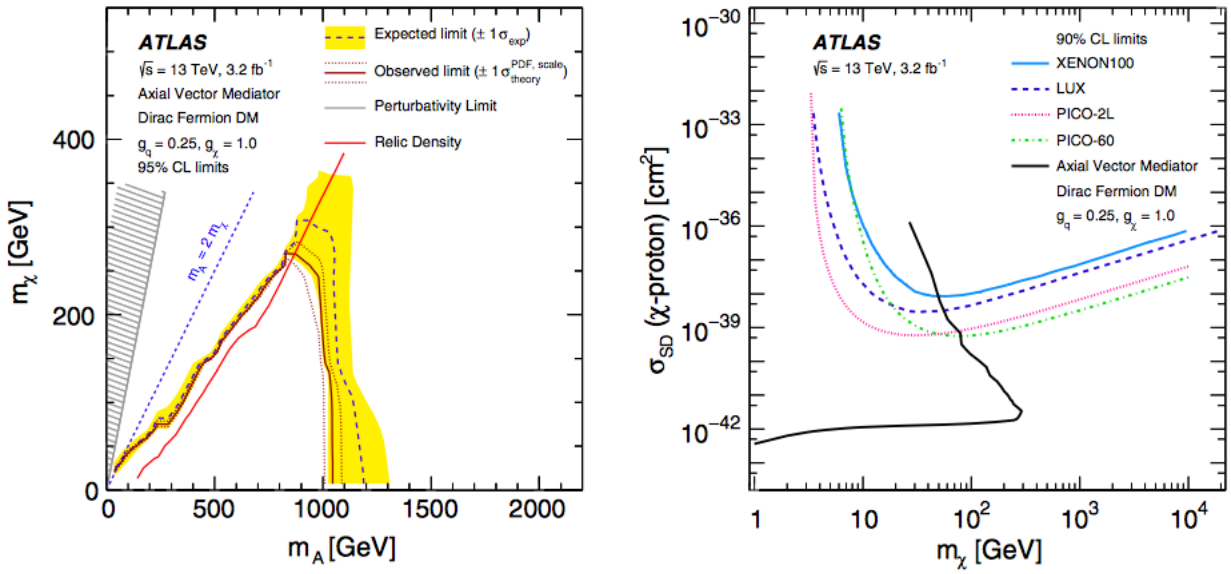

Figure 4: Left: Inferred 95% C.L. contours in the m_χ – m_A parameter plane. The solid (dashed) curve shows the median of the observed (expected) limits while the band indicate the $\pm 1\sigma$ uncertainty. Right: a comparison of the inferred limits (at 90% C.L.) to the constraints from direct detection experiments on the spin-dependent WIMP-proton scattering cross section in the context of a simplified model with axial-vector couplings. The comparison is model dependent and solely valid in the context of this model, assuming minimal mediator width and the coupling values $g_q = 1/4$ and $g_\chi = 1$. Figures from ATLAS Collaboration, PRD 94, 032005, 2016 or arXiv:1604.07773

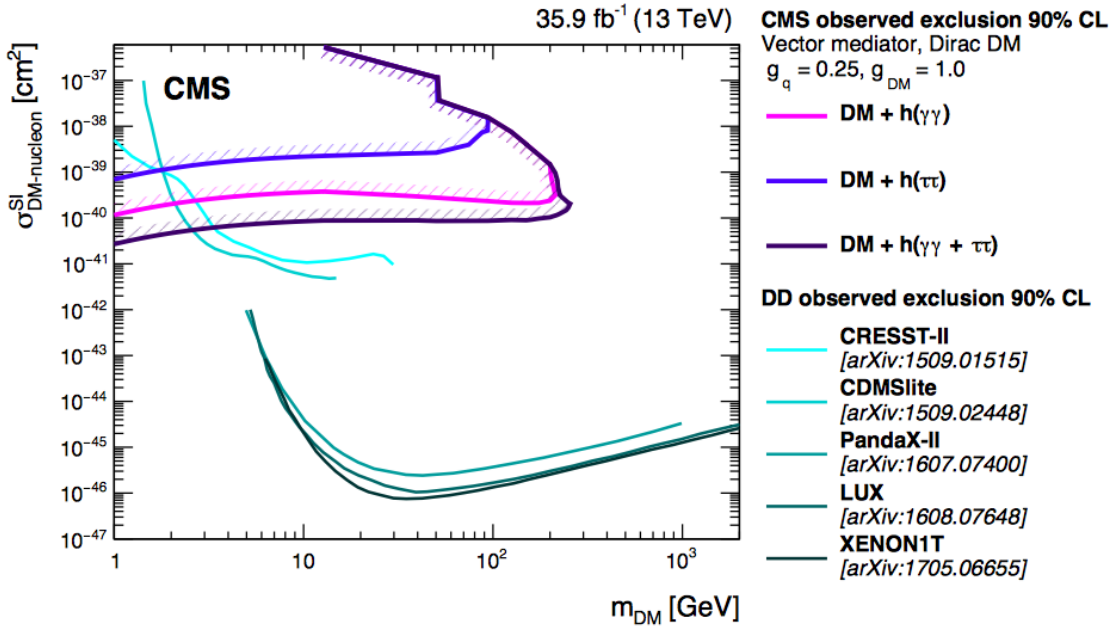

Figure 5: The 90% CL exclusion limits on the DM-nucleon SI scattering cross section as a function of m_{DM}. Results obtained in this analysis are compared with those from a selection of direct detection experiments. The latter exclude the regions above the curves. Limits from CDMSLite, LUX, XENON-1T, PandaX-II, and CRESST-II are shown. Figure from CMS, JHEP 09 (2018) 046 and arXiv:1806.04771